

A comparative investigation of mechanical and tribological properties of multilayered CVD-diamond coatings: effect of boron doping

Kaleem Ahmad Najar^{1*}, Nazir Ahmad Sheikh¹, M. A. Shah^{2*}

¹ Department of Mechanical Engineering, National Institute of Technology Srinagar 190006, India

² Department of Physics, National Institute of Technology Srinagar 190006, India

*Corresponding author: Tel: (+91) 9906578851, 9419018195; Email: najar.kaleem@gmail.com, shah@nitsri.net

Received: 26 June 2016, Revised: 04 November 2016 and Accepted: 20 November 2016

DOI: 10.5185/amlett.2017.6959

www.vbripress.com/aml

Abstract

In the present work, smooth boron-doped (BD) and undoped multilayered diamond coating systems (MDCS) with top layer nanocrystallinity were deposited on chemically etched cemented tungsten carbide (WC-6%Co) substrates, using hot filament chemical vapour deposition (HFCVD) technique. Both coatings were accomplished by combining the alternate thin films of microcrystalline diamond (MCD) and nanocrystalline diamond (NCD) with a transition layer (TL) of $\sim 1\mu\text{m}$ thick, using predetermined process parameters during the deposition process. The effects of boron doping on the residual stresses (σ), hardness (H) and coefficient of friction (COF) of MDCS were analyzed using Raman spectroscopy, Berkovich Nanoindenter and Micro-tribometer, respectively. The comparison has been documented between BD-MDCS with undoped one, under same input operating conditions and within same atmospheric conditions. The frictional characteristics were studied under the application of increasing normal load when sliding against smooth alumina (Al_2O_3) ceramic counter ball for the total duration of 20 min, within dry sliding conditions. The average values of COF of undoped-MDCS and BD-MDCS decrease from $\sim 0.30 - 0.27$ and $\sim 0.28 - 0.25$, respectively under the application of 1 – 10 N loads. Also, the average values of indentation depths for undoped-MDCS and BD-MDCS were ~ 65 nm and ~ 70 nm, with average hardness values in the range of $\sim 65 - 80$ GPa and $\sim 55 - 75$ GPa, respectively. Therefore, depositing smooth, adhesive and thick BD-multilayered diamond coatings on cemented tungsten carbide components would certainly enable its many useful future applications in mechanical industry. Copyright © 2017 VBRI Press.

Keywords: Multilayered CVD-diamond coatings, boron doping, nanoindentation, coefficient of friction, tribo-layer.

Introduction

Chemical vapour deposition (CVD) diamond coatings have a combination of excellent mechanical and tribological properties, such as extremely high hardness, exceptional wear resistance, and a low COF, sliding against many counter bodies including ceramics and metals [1]. CVD-diamond coatings have attracted great interests to be used as protective and wear-resistant film on mechanical bearings and seals in rotary machines [2-4]. Depositing CVD-diamond coatings on hard tools like WC-Co essentially increase their durability during heavy cutting or milling operations [5]. However, the presence of surface cobalt (Co) on the WC-Co material resists diamond nucleation and allows the formation of graphitic carbon phases, which decreases the strength of adhesion between coating and substrate [6]. Therefore, the removal of surface cobalt by chemical etching technique is an important step to increase this force of adhesion [7].

The grain size of the diamond films was mainly controlled by methane concentration and chamber

pressure thus, CVD-diamond coatings are mainly classified into nanocrystalline diamond (NCD) and microcrystalline diamond (MCD) on the basis of their grain sizes [8]. Smooth NCD films increases the tribological properties of mechanical components, but with the decreasing grain size the intrinsic residual stresses increase within a layer. Also, the presences of large number of grain boundaries in NCD films are the source of graphitic carbon phases, which affects their crystallinity as well as the mechanical properties [9, 10]. NCD coatings show low hardness, low elastic modulus, low COF and high adhesiveness (on WC-Co), whereas; MCD coatings show high hardness, high elastic modulus, high COF and low adhesiveness (on WC-Co) [11].

A new deposition technique called multilayered diamond coating system (MDCS) was designed to improve the adhesion factor, hardness value and wear resistance of mechanical components by joining the advantages of both MCD and NCD types of coatings, with a transition layer (TL) between them using HFCVD

process [12]. For the enhancement of wear resistance of mechanical tools during practical applications, the adhesion between the coating and substrate is an important parameter, but the MCD coating has good load bearing capacity as compared to NCD coating [13]. The MDCS has been used for the purpose of prevention of enormous MCD grain growth, to enhance the fracture toughness [14-16] and to reduce the magnitude of residual stresses within the coating [17]. MDCS have shown excellent adhesion strength as compared to single-layer NCD coating and to have the smallest average grain sizes [18]. However, the interface between two diamond layers in MDCS plays an important role on the mechanical behaviour during industrial applications and their excellent wear resistance was achieved due to the high adhesion between MCD and NCD interfaces [19]. The MDCS is also well known to improve the tribological characteristics of ceramics, carbides and hard metals, by increasing the adhesion between the coating and the substrate, allowing higher applied loads, reduction of residual thermal stresses and improving force of delamination [20].

In this work, smooth and adhesive thin undoped and BD-MDCS were deposited on chemically etched WC-Co substrates with uniform thickness of $\sim 3\mu\text{m}$ each, using HFCVD technique. Systematic investigation of the relationship between applied increasing load and COF was carried out to better understand the tribological behaviour of undoped-MDCS & BD-MDCS. The results may serve breakthrough information for the designer to design the mechanical component using this novel coating procedure.

Experimental

Materials and methods

Cemented tungsten carbide (WC-Co: CERATIZIT-CTF12A grade) with 6% Co & 0.8-1.3 μm WC grain size) was selected as the substrate material in order to minimize the residual compressive stress developed during deposition process. WC-Co substrates of size 1cm \times 1cm \times 0.3cm and with surface roughness factor (Ra) of $\sim 0.35\mu\text{m}$ were cleaned in ethyl alcohol with ultrasonic agitation to remove the impurities from the surface. From the Co-cemented tungsten carbide sample the surface cobalt was removed using standard chemical etching technique to increase the adhesiveness factor of coating on the substrate. MDCS (undoped & BD) were successfully deposited on chemically etched WC-Co substrates, using HFCVD technique with uniform thickness of $\sim 3\mu\text{m}$. The boron content is formed when trimethyl borate ($\text{C}_3\text{H}_9\text{BO}_3$) is dissolved in acetone solution and the mixed solution in the liquid container is introduced in the reactor by part of H_2 .

Structural characteristics of these coatings were studied using grazing incidence X-ray diffraction (PANalytical) technique with Cu K α ($\lambda = 0.154\text{ nm}$) radiation at 3 $^\circ$ grazing angle and confocal Raman microscope (Alpha 300R, WITec) at an excitation wavelength of 448nm. Surface morphology of these coatings were studied using

a high-resolution scanning electron microscope (HRSEM, Quanta 3D, FED). Nanoindentation tests were conducted using triboindenter (TI 950, HYSITRON) with a Berkovich tip of total included angle (2α) = 130.5 $^\circ$, radius of curvature approximately 150nm and at 10mN trapezoidal load cycle. The values of hardness (H) were calculated from the load-displacement data and the values of elastic modulus (E) were calculated using Oliver and Pharr mathematical procedure [21]. Friction characteristics were carried out using a ball-on-disc type linear reciprocating micro-tribometer (CSM Instruments, Switzerland) under dry sliding conditions. Smooth alumina (Al_2O_3) ceramic ball of size $\varnothing 6\text{mm}$ was used as sliding body, when applying normal loads of 1N, 5N & 10N. A sliding speed of 8cm/s, frequency of 2Hz and a friction stroke length of 5mm were used for the total duration of 20 min. The detailed input experimental tribological operating conditions are listed in Table 1.

Table 1. Input operating tribological conditions.

S. No.	Parameters	Operating conditions
1	Normal Load	1, 5 & 10 N
2	Sliding Velocity	8 cm/s
3	Relative Humidity	60 (± 5) %
4	Sliding Time	20 minutes
5	Surface Condition	Dry
6	Materials Tested	MDCS & BD-MDCS
7	Ball Material	Alumina (Al_2O_3)
8	Diameter of ball	6 mm
9	Stroke length	5 mm
10	Frequency	2Hz
11	Temperature	30 \pm 1 $^\circ\text{C}$
12	Roughness Factor	
	(Ra):	
	NCD	$\sim 0.19\mu\text{m}$
	BDNCD	$\sim 0.12\mu\text{m}$

Method of deposition

Hot filament CVD system (Model 650 series, sp3 Diamond Technologies) with excellent process control unit was used for the deposition of diamond films, using growth rate of 1 $\mu\text{m/hr}$. Deposition parameters such as chamber pressure and methane concentration were controlled easily during the experiment by using throttle valve and mass flow controllers, respectively. Hydrogen (H_2) and methane (CH_4) were used as the precursor gases and their flow rates were completely controlled using mass flow controllers. An array of tungsten wires ($\varnothing 0.12\text{ mm}$) in systematic order were used as hot filaments for the activation of these precursor gases. The distance between filament and substrate was kept 15mm for all the experiments. The grain size of the diamond films was usually controlled by methane concentration and chamber pressure. By increasing the methane concentration and decreasing the chamber pressure gives the growth of secondary nucleation and therefore decreases the grain size from MCD to that of NCD [8]. The toxic by-product gases or exhaust gases produced after the deposition process from the HFCVD chamber were diluted using nitrogen (N_2) gas. However, these N_2

gases were used before and after the diamond growth process to flush the chamber. CVD-chamber was made of aluminum with cooling channels and the temperature of the chamber was maintained at $\sim 50^\circ\text{C}$ using a circulating water chiller. Both coatings were designed by combining the alternate MCD and NCD layers with a transition layer (TL) of $\sim 1\ \mu\text{m}$ thickness, they are; undoped-MDCS (MCD-TL-NCD) and BD-MDCS (MCD-TL-BDNC). This transition layer was actually formed by linear change of process parameters from microcrystallinity to nanocrystallinity [22]. However, in case of BD-MDCS, a small content of boron ($\sim 0.35\%$) was added to the NCD surface for modifications in mechanical and tribological properties. The growth parameters used for the deposition of MCD, NCD and BD-NCD coatings are listed in **Table 2**.

Table 2. Growth parameters used for the deposition of MCD, NCD & BD-NCD coatings.

Coating Type	Process Pressure (Torr)	CH ₄ /H ₂ Ratio (%)	Filament Temperature (°C)	Substrate Temperature (°C)	Boron Concentration (%)	Duration (hrs)
MCD	36	2	2200	800-850	-	1
NCD	12	4	2200	800-850	-	1
BD-NCD	12	4	2200	800-850	-0.35	1

Results and discussions

In the present experimental work, the frictional characteristics of undoped-MDCS & BD-MDCS were compared when sliding against smooth Al₂O₃ ball, under the application of increased normal load, using ball-on-disc type linear reciprocating micro-tribometer. Experiments were conducted at normal loads of 1, 5 and 10 N, sliding velocity 8 cm/s, stroke length 5mm, frequency = 2 Hz, temperature $30 \pm 1^\circ\text{C}$, sliding time 20 min and relative humidity $\sim 65\%$ under dry sliding conditions. Nanoindentation tests of these CVD-diamond coatings were conducted using Berkovich nanoindenter and their hardness values were calculated from the load-displacement data. The elastic modulus values were calculated, using Oliver and Pharr mathematical method as [21]:

$$\text{Harness (H)} = P/A = P/24.5 h_c^2 \text{ and} \quad (1)$$

$$\text{Stiffness (S)} = dP/dh = 2E^* (\sqrt{\pi}/2\sqrt{A})$$

$$\text{Elastic modulus (E)} = (\text{slope of the elastic unloading curve}) \times (\sqrt{\pi}/2\sqrt{A}) \quad (2)$$

$$\text{Reduced modulus, } 1/E^* = 1-\nu^2/E + 1-\nu^2/\acute{E} \quad (3)$$

$$E^* = dP/dh (1/2h_c) (1/\beta) [\sqrt{\pi}/24.5] \quad (4)$$

$$A = 3 (\sqrt{3} h_c^2) \tan^2 (65.3) = 24.5 h_c^2 \text{ and} \quad (5)$$

$$\beta = 1.034 \text{ for Berkovich indenter}$$

where, P= maximum load, A= area of contact, h_c is the contact depth, E = elastic modulus of specimen & \acute{E} = elastic modulus of indenter.

Physical characterizations

Raman spectroscopy and residual stress analysis of MDCS

Raman spectroscopy was used to check the chemical structure and crystallinity of the diamond coatings and if the crystalline diamond coating shows a fundamental Raman peak at approximately $1333\ \text{cm}^{-1}$, confirms that the coating is diamond in nature [23]. **Fig.1. (a, b)** show the Raman spectra of the top-layer surfaces corresponding to undoped-MDCS and BD-MDCS, respectively. In **Fig. 1 (a)**, the characteristic fundamental Raman peak of undoped-NCD exists at $1336\ \text{cm}^{-1}$ and this shift of the fundamental Raman peak towards higher side of $1333\ \text{cm}^{-1}$, confirms the presence of residual compressive stresses. Mainly, these residual compressive stresses exist due to the difference in thermal expansion coefficients between substrate and coating [24]. Residual stresses can be calculated from $\sigma = -0.348 (v_m - v_0)$ GPa for the fundamental Raman peak at $v_m = 1336\ \text{cm}^{-1}$ & $v_0 = 1332\ \text{cm}^{-1}$ [25]. Thus, undoped-NCD coating contains compressive stresses of -1.4GPa , where negative sign indicates compressive stress. Two other peaks $v_1 = 1141\ \text{cm}^{-1}$ & $v_3 = 1491\ \text{cm}^{-1}$, are characteristics of in-plane (C-H) and stretching (C=C) vibrational modes, respectively. The existence of these modes was ascribed to the formation of transpolyacetylene (TPA) chain in the grain boundaries in case of NCD coating [26]. For BD-NCD coating, the characteristic fundamental Raman peak at $1336\ \text{cm}^{-1}$ shifts to lower value at $1300\ \text{cm}^{-1}$ due to the slightly boron doping, and the other peak at $1516\ \text{cm}^{-1}$ shows the presence of graphitic carbon phases (G-band). Hence this downshift of the fundamental Raman peak is due to the result of the breakdown of the $k = 0$ selection rule due to boron doping. The two other peaks around $459\ \text{cm}^{-1}$ and $1213\ \text{cm}^{-1}$ represent the actual boron incorporation in the lattice [27]. The residual tensile stress for the BD-NCD coating can be also calculated as, $\sigma = -0.348 (1300-1332) = 11.13\ \text{GPa}$, where positive sign implies tensile stress.

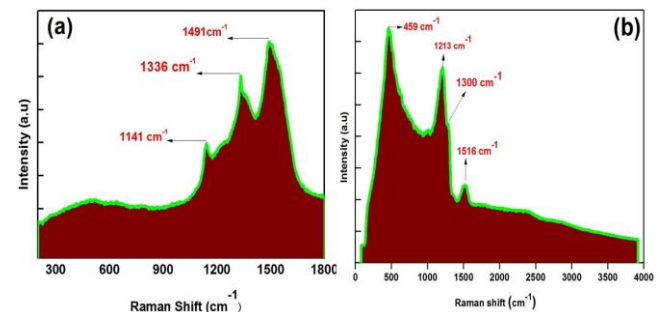


Fig.1 Raman spectra of the MDCS with (a) undoped-NCD & (b) BD-NCD.

X-ray diffraction (XRD) patterns of MDCS

The XRD pattern of the top-layer surface corresponding to MDCS is shown in **Fig. 2**. Sharp and strong peaks of cubic diamond coatings were observed at (111) crystal & (220) crystal planes at the diffraction angles of 44° & 75.5° respectively, along with the substrate (WC) peaks.

These diamond peaks confirm the crystallinity of the NCD coating. The highest peaks of WC substrate confirm that the grain size of tungsten carbide is more than diamond coating. However, with the addition of boron content the grain size and thus, lattice parameters of diamond films were changed. Therefore, using the equations given by Brunet [28], the change of lattice constant for BDNCD film can be calculated as:

$$\Delta a/a = \beta [B] \tag{6}$$

where, $\Delta a = a - a_0$, $a_0 = 3.5619 \text{ \AA}$ for undoped-diamond film, $a = a_0 + \Delta a = (3.5619 + \Delta a) \text{ \AA}$ for BD- diamond film, and $[B] = 0.35$ is the concentration per unit volume of the boron atoms.

$$\beta (\text{cm}^3) = 3.87 \times 10^{-25} + 3.73 \times 10^{-45} [B] \tag{7}$$

From eq. (7), $\beta (\text{cm}^3) = 3.87 \times 10^{-25}$ & from eq. (6), $\Delta a/a = 3.87 \times 10^{-25} \times [0.35] = 1.3545 \times 10^{-25}$.

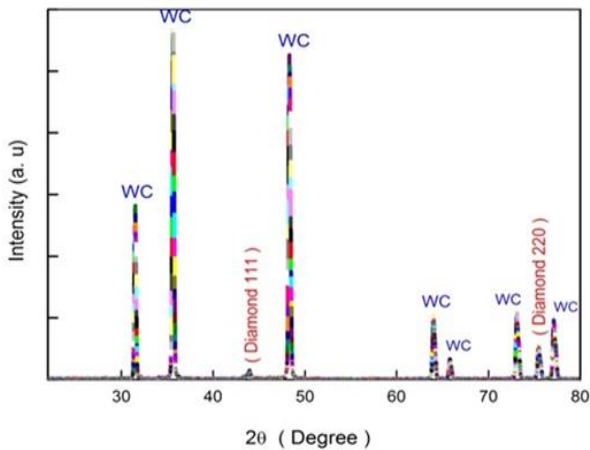


Fig. 2. X-ray diffraction patterns of the MDCS.

Surface morphology of MDCS

Scanning electron microscopy (SEM) technique was used to study the surface morphology, microstructure and grain size of the diamond coatings. As per the earlier studies it is already mentioned that during the diamond deposition process increase in methane concentration leads to secondary nucleation, and therefore changes the nature of the grains from microcrystalline to nanocrystalline. The cauliflower type of morphology is generally shown by the top-layer surface (NCD) corresponding to MDCS as per the earlier reports [29], shown in Fig. 3(a, b). However, Fig. 3(c) shows the cross-sectional morphology of the MDCS along with the thickness of both coating and substrate. The compositional analysis of the NCD surface was confirmed using energy dispersive spectroscopy (EDS), as shown in Fig. 3(d).

Nanoindentation and hardness measurement of MDCS

Before nanoindentation tests these CVD-diamond coatings were polished against Si₃N₄ pin for the duration of 2 hrs using a tribometer. Fig. 4(a, b) show the load-displacement curves corresponding to 5 indentations carried out on undoped-MDCS and BD-MDCS,

respectively. The average indentation depth for undoped-MDCS was ~65 nm, whereas for BD-MDCS, it was ~70 nm. The hardness values (H) of undoped-MDCS were in the range 65 – 80 GPa and these values resembles approximately with the recent research work done on CVD-diamond coatings [22]. However, the hardness values of BD-MDCS were slightly decreased in the range of 55 – 75 GP.

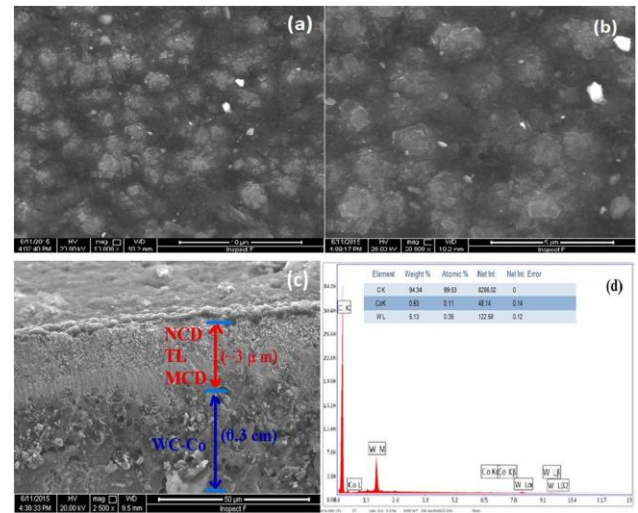


Fig. 3. (a, b) Surface morphology of the MDCS, (c) Cross-sectional morphology of coating-substrate system & (d) EDS of the MDCS.

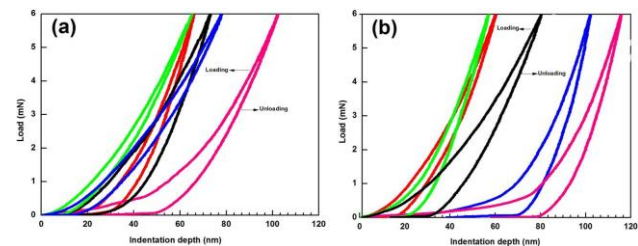


Fig. 4. Load-displacement curves corresponding to 5 indentations on MDCS with (a) undoped-NCD & (b) BD-NCD.

Friction characteristics of MDCS

Since, limited research has been done on boron doped (BD) diamond films; however, some of the important literature related to this novel coating method is mentioned here: an appropriate amount of boron dopant on diamond films will refine diamond grains; increases grain size, change nature of residual stresses and improve film quality. BD-diamond films present tensile residual stresses while undoped-diamond films show compressive residual stresses. However, during friction measurement the BD-diamond films shown low COF as compared to undoped-diamond films, although BD-diamond films have mostly larger grain size and rougher surface. Boron doping also improves the wear resistance of diamond films and also their adhesive strength on the substrates [30, 31]. Also the boron incorporation between diamond grains in CVD-diamond layer would reduce the purity and quality of thin diamond films to some extent, but resulting

in lower hardness and Young's modulus of BD-diamond coating compared with undoped-diamond coating [32].

In this study, the frictional characteristics of undoped-MDCS and BD-MDCS were studied, when sliding against smooth Al₂O₃ ceramic ball, using ball on disc-Micro-tribometer with increasing normal load and for the total duration of 20 min. **Fig. 5 (a)** shows the variation of average COF of undoped-MDCS under the application of 1–10N load, whereas **Fig. 5 (b, c, d)** show individually the variation of COF with the sliding time at 1, 5 & 10N loads, respectively. The average value of COF on the surface of undoped-MDCS decreases from ~0.30 – 0.29 and then 0.29 – 0.27, by increasing the normal load from 1 – 10 N. **Fig.6 (a)** shows the variation of average COF of BD-MDCS under same input operating conditions, whereas **Fig. 6 (b, c, d)** show individually the variation of COF with the sliding time at 1, 5 & 10N loads, respectively. Similarly, the average value of COF on the surface of BD-MDCS decreases from ~0.28 – 0.27 and then 0.27 – 0.25, by increasing the normal load from 1 – 10 N.

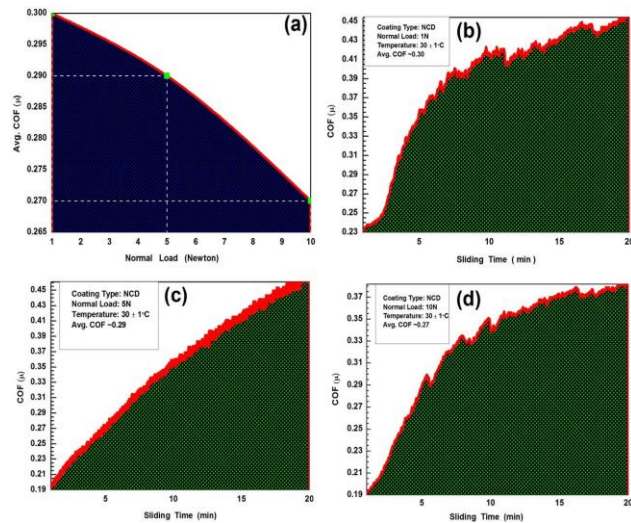


Fig. 5. Variation of COF of undoped-MDCS sliding against Al₂O₃ ball with respect to (a) Normal load, and sliding time at (a) 1N, (b) 5N & (c)10N load.

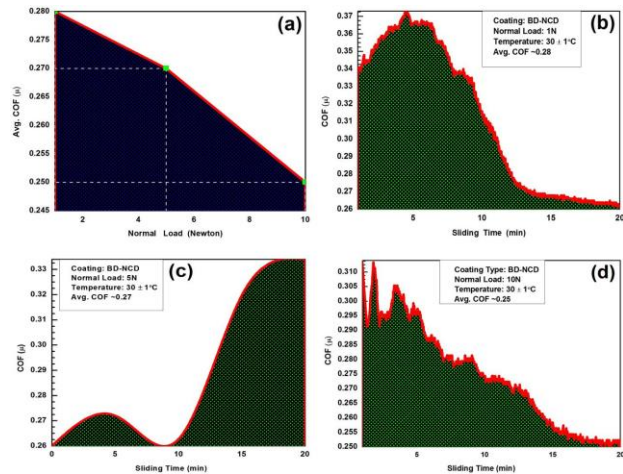


Fig. 6. Variation of COF of BD-MDCS sliding against Al₂O₃ ball with respect to (a) Normal load, and sliding time at (a) 1N, (b) 5N & (c)10N load.

There may be many explanations regarding this behavior of decreasing COF of CVD-diamond films: one possible reason for low COF of BD-diamond films compared with undoped diamond films is that the interaction mechanism between two contact surfaces was changed because of boron incorporation. Since, the existence of boron carbide and boron hydride chemical bonds would help change the surface frictional energy dissipation and thus change the COF. The other possible reason for low COF of BD-diamond films compared with undoped diamond films is that, the low COF combined with the increased thermal stability under oxidizing environment conditions. Also, the oxide generated during friction may serve as solid lubrication, which will help to decrease COF for BD-diamond films [27, 33].

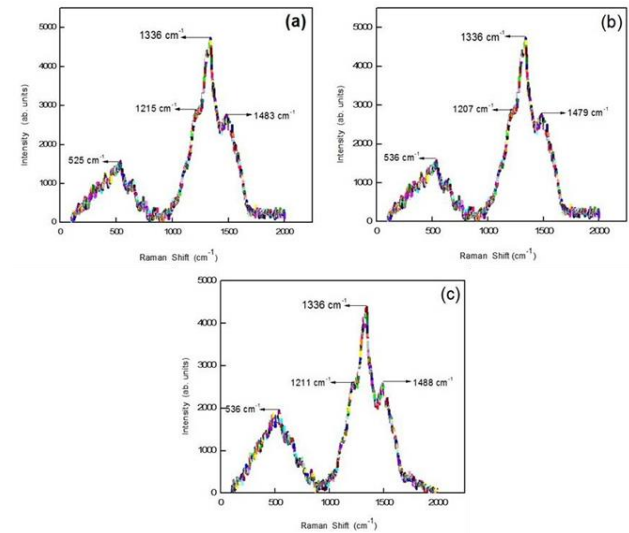


Fig. 7. Raman spectra of the wear track obtained on BD-MDCS when sliding against Al₂O₃ ball at (a) 1N, (b) 5N & (c) 10N load.

Characterizations of the wear-tracks formed on CVD-diamond coatings after friction measurement

Fig. 7 (a, b, c) show the Raman spectra of the wear tracks formed on the surface of BD-MDCS at 1 N, 5 N & 10 N loads respectively, when sliding against smooth Al₂O₃ ball after friction measurement. The existence of residual compressive stresses in all these wear tracks are estimated from $\sigma = -0.348 (v_m - v_0)$ GPa, for the main fundamental Raman peak at $v_m = 1336 \text{ cm}^{-1}$ & $v_0 = 1333 \text{ cm}^{-1}$. Therefore, each wear track of BD-MDCS contains residual compressive stresses of 1.044 GPa, under the application of each load. Thus, after friction measurement the residual tensile stresses of BD-MDCS changed to compressive stresses with the decrease in magnitude, but remained same under the application of increasing normal load. The other peaks around 525 cm⁻¹, 536 cm⁻¹ and 536 cm⁻¹ at the extreme left side of fundamental diamond peak (1336 cm⁻¹) as shown in **Fig. 7 (a, b, c)** respectively, represent the actual boron incorporation to the top-layer surface. The other two modes (v_1 & v_3) on left and right sides of fundamental diamond peak at each load, represent the change in-plane (C-H) and stretching (C=C)

vibrational modes respectively, and the variations in these peaks occurred due to changing load.

However, all CVD-diamond coatings undergo phase transformation during long-duration of rubbing, high-load (high-speed) sliding tests, and then the transformation products trapped at the sliding interfaces can periodically influence the friction and wear performance [34]. **Fig. 8 (a)** shows surface morphology of the wear-track formed on the surface of MDCS and **Fig 8(b)** shows the compositional analysis of the tribo-layer formed on the wear-track of Al₂O₃ counter ball after sliding against CVD-diamond coatings, using energy dispersive spectroscopy (EDS) technique, respectively. Also, the detailed mechanical and tribological experimental results are listed in **Table 3**.

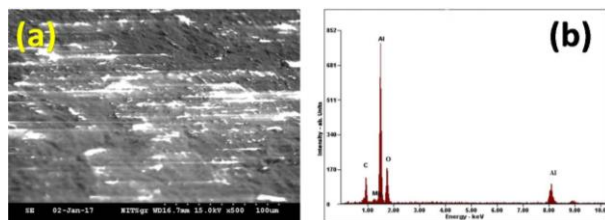


Fig. 8. Surface morphology of Al₂O₃ counter ball after sliding against diamond surfaces with (a) SEM image and (b) EDS analysis.

Table 3. Experimental mechanical & tribological results.

Coating Type	Residual Stresses (σ)	Indentation Depth (h)	Hardness Values (H)	Elastic Modulus (E)	Variation of COF
Undoped-MDCS	-1.4 GPa	~65 nm	~65-80 GPa	~1100 GPa	~0.30 - 0.27
BD-MDCS	11.14 GPa	~70 nm	~55-75 GPa	~1050 GPa	~0.28 - 0.25

Conclusion

The effect of boron-doping on the lattice parameter, residual stresses, hardness and frictional characteristics of multilayered-diamond coating system were analyzed experimentally here. However, incorporating low boron concentration of 0.35% into top-layer surface of MDCS, the fundamental characteristic diamond peak at 1336 cm⁻¹ downshift to 1300 cm⁻¹ and the compressive residual stresses were changed to tensile stresses. It was also observed that the average hardness values of MDCS were slightly decreased due to boron-doping and the BD-MDCS shows less value of COF than undoped one. Further, it was also estimated that using boron content of about ~0.35%, there was nearly 8% reduction in COF, ~7.14% increment in indentation depth and ~9.7% reduction in hardness. Hence, all the experimental tribological results conclude that COF of both undoped-MDCS and BD-MDCS decrease with the increase in the magnitude of load, as like other types of diamond coatings.

Acknowledgments

The Authors would like to thank MSRC lab (IIT Madras) for the deposition of coatings and Surface Engineering Division (NAL, Bangalore, India) for tribological test study and Department of Physics

and Department of Mechanical Engineering, National Institute of Technology, Hazratbal Srinagar, J&K India their assistance during experimental work.

Authors' contributions

Kaleem Ahmad Najar and M. A. Shah contributed in the synthesis and characterization and drafted the manuscript. All authors read and approved the final manuscript.

Notation

BD	Boron-doped
NCD	Nanocrystalline diamond
MCD	Microcrystalline diamond
MDCS	Multilayered diamond coating system
TL	Transition layer
HFCVD	Hot filament chemical vapour deposition
σ	Residual stress
H	Hardness
h	Indentation depth
E	Elastic modulus
COF	Coefficient of friction
XRD	X-ray diffraction
SEM	Scanning electron microscopy
EDS	Energy dispersive spectroscopy

References

- Xuelin Lei; Bin Shen; Sulin Chen; Liang Wang; Fanghong Sun; *Tribology International*, **2014**, 69, 118.
DOI: [10.1016/j.triboint.2013.09.012](https://doi.org/10.1016/j.triboint.2013.09.012)
- A. Sumant; A. Krauss; D. Gruen; O. Auciello; A. Erdemir; M. Williams; *Tribology Transactions*, **2005**, 48, 24.
- P. Hollman; H. Björkman; A. Alahelisten; S. Hogmark; *Surface & Coatings Technology*, **1998**, 105, 169.
DOI: [S0257-8972\(98\)00481-2](https://doi.org/10.1016/S0257-8972(98)00481-2)
- M. Perle; C. Bareiss; S. Rosiwal; R. Singer; *Diamond & Related Materials*, **2006**, 15, 749.
DOI: [10.1016/j.diamond.2005.10.069](https://doi.org/10.1016/j.diamond.2005.10.069)
- R. Haubner; B. Lux; *Int. J. of Refractory Metals & Hard Materials*, **1996**, 14, 111.
- Htet Sein; Waqar Ahmed; Mark Jackson; Robert Woodward; Riccardo Polini; *Thin Solid Films*, **2004**, 447, 455.
DOI: [10.1016/j.tsf.2003.08.044](https://doi.org/10.1016/j.tsf.2003.08.044)
- N. M. Everitt; R. F. Silva; J. Vieira; C. A. Rego; C. R. Henderson; P.W. May; *Diamond & Related Materials*, **1995**, 4, 730.
- M. Ali; M. Ürgen; *Applied Surface Science*, **2011**, 257, 8420.
DOI: [10.1016/j.apsusc.2011.04.097](https://doi.org/10.1016/j.apsusc.2011.04.097)
- D. Schwarzbach; R. Haubner; B. Lux; *Diamond & Related Materials*, **1994**, 3, 757.
DOI: [10.1016/0925-9635\(94\)90264-X](https://doi.org/10.1016/0925-9635(94)90264-X)
- M. Wiora; K. Brühne; A. Flöter; P. Gluche; T. M. Willey; S.O. Kucheyev; *A.W. Van Buuren; A.V. Hamza; J. Biener; H.-J. Fecht; Diamond & Related Materials*, **2009**, 18, 927.
DOI: [10.1016/j.diamond.2008.11.026](https://doi.org/10.1016/j.diamond.2008.11.026)
- Fanghong Sun; Yuping Ma; Bin Shen; Zhiming Zhang; Ming Chen; *Diamond & Related Materials*, **2009**, 18, 276.
DOI: [10.1016/j.diamond.2008.10.064](https://doi.org/10.1016/j.diamond.2008.10.064)
- R. H. Dauskardt; M. Lane; Q. Ma; N. Krishna; *Engineering Fracture Mechanics*, **1998**, 61, 141.
DOI: [S0013-7944\(98\)00052-6](https://doi.org/10.1016/S0013-7944(98)00052-6)
- F. A. Almeida; M. Amaral; F. J. Oliveira; A. J. S. Fernandes; R. F. Silva; *Vacuum*, **2007**, 81, 1443.
DOI: [10.1016/j.vacuum.2007.04.008](https://doi.org/10.1016/j.vacuum.2007.04.008)
- L. Schafer; M. Höfer; R. Kröger; *Thin Solid Films*, **2006**, 515, 1017.
DOI: [10.1016/j.tsf.2006.07.073](https://doi.org/10.1016/j.tsf.2006.07.073)
- S. Takeuchi; S. Oda; M. Murakawa; *Thin Solid Films*, **2001**, 398, 238.
DOI: [S0040-6090\(01\)01499-7](https://doi.org/10.1016/S0040-6090(01)01499-7)
- N. Jiang; K. Sugimoto; K. Nishimura; Y. Shintani; A. Hiraki; *Journal of Crystal Growth*, **2002**, 242, 362.
DOI: [S0022-0248\(02\)01443-4](https://doi.org/10.1016/S0022-0248(02)01443-4)

17. S. A. Catledge; J. Borham; Y. K. Vohra; W. R. Lacefield; J. E. Lemons; *Journal of Applied Physics*, **2002**, *91*, 5347.
DOI: [10.1063/1.1464233](https://doi.org/10.1063/1.1464233)
18. Leigh Booth; A. Shane Catledge; Dustin Nolen; G. Raymond Thompson; K. Yogesh Vohra; *Materials*, **2011**, *4*, 857.
DOI: [10.3390/ma4050857](https://doi.org/10.3390/ma4050857)
19. A. Flávia Almeida; Ermelinda Salgueiredo; J. Filipe Oliveira; F. Rui Silva; L. Daniel Baptista; B. Suzana Peripolli; A. Carlos Achete; *ACS Applied Materials & Interfaces*, **2013**, *5*, 11725.
DOI: [10.1021/am403401s](https://doi.org/10.1021/am403401s)
20. E. Salgueiredo; C. S. Abreu; M. Amaral; F. J. Oliveira; J. R. Gomes; R. F. Silva; *Wear*, **2013**, *303*, 225.
DOI: [10.1016/j.wear.2013.03.049](https://doi.org/10.1016/j.wear.2013.03.049)
21. W. C. Oliver; G. M. Pharr; *Journal of Materials Research*, **1992**, *7*, 1564.
22. Ravikumar Dumpala; Maneesh Chandran; N. Kumar; S. Dash; B. Ramamoorthy; M. S. Ramachandra Rao; *International Journal of Refractory Metals & Hard Materials*, **2013**, *37*, 127.
DOI: [10.1016/j.ijrmhm.2012.11.007](https://doi.org/10.1016/j.ijrmhm.2012.11.007)
23. S. Praver; R. J. Nemanich; *Philos. Trans. R. Soc. Lond. A*, **2004**, *362*, 2537.
DOI: [10.1098/rsta.2004.1451](https://doi.org/10.1098/rsta.2004.1451)
24. J. Gunnars; A. Alahelsten; *Surface & Coatings Technology*, **1996**, *80*, 303.
DOI: [0257-8972 \(95\) 02436-0](https://doi.org/10.1016/S0257-8972(95)02436-0)
25. Maneesh Chandran; C.R. Kumaran; S. Gowthama; P. Shanmugam; R. Natarajan; S. S. Bhattacharya; M. S. Ramachandra Rao; *International Journal of Refractory Metals & Hard Materials*, **2013**, *37*, 117.
DOI: [10.1016/j.ijrmhm.2012.11.005](https://doi.org/10.1016/j.ijrmhm.2012.11.005)
26. H. Kuzmany; R. Pfeiffer; N. Salk; B. Günther; *Carbon*, **2004**, *42*, 911.
DOI: [10.1016/j.carbon.2003.12.045](https://doi.org/10.1016/j.carbon.2003.12.045)
27. Qi Liang; Andrei Stanishevsky; K. Yogesh Vohra; *Thin Solid Films*, **2008**, *517*, 800.
DOI: [10.1016/j.tsf.2008.08.171](https://doi.org/10.1016/j.tsf.2008.08.171)
28. F. Brunet; A. Deneuve; P. Germi; M. Pernet; E. Gheeraert; *Applied Physics Letters*, **1997**, *81*, 1120.
DOI: [10.1063/1.363856](https://doi.org/10.1063/1.363856)
29. W. Kulisch; C. Popov; *Physics Status Solidification A*, **2006**, *203*, 203.
30. Zhaozhi Liu; Feng Xu; Junhua Xu; Xiaolong Tang; Ying Liu; Dunwen Zuo; *International Journal of Chemical, Nuclear, Materials & Metallurgical Engineering*, **2015**, *9*, 577.
DOI: [1999.2/10001006](https://doi.org/10.1002/10001006)
31. Liang Wang; Xuelin Lei; Bin Shen; Fanghong Sun; Zhiming Zhang; *Diamond & Related Materials*, **2013**, *33*, 54.
DOI: [10.1016/j.diamond.2013.01.004](https://doi.org/10.1016/j.diamond.2013.01.004)
32. C. Yan; H. Mao; W. Li; J. Qian; Zhao, Y. Zhao; R. J. Hemley; *Phys. Status Solidi.*, **2004**, *201*, R25.
DOI: [10.1002/pssa.200409033](https://doi.org/10.1002/pssa.200409033)
33. Qi Liang; A. Shane Catledge; K. Yogesh Vohra; *Mater. Res. Soc. Symp. Proc.*, **2004**, *791*, Q 8.19.1.
34. A. Erdemir; G. R. Fenske; A. R. Krauss; D. M. Gruen; T. McCauley; R. T. Csencsits; *Surface & Coatings Technology*, **1999**, *120*, 565.
DOI: [S0257-8972 \(99\) 00443-0](https://doi.org/10.1016/S0257-8972(99)00443-0)



A Monthly Journal

Publish your article in this journal

Advanced Materials Letters is an official international journal of International Association of Advanced Materials (IAAM, www.iaamonline.org) published monthly by VBRI Press AB from Sweden. The journal is intended to provide high-quality peer-review articles in the fascinating field of materials science and technology particularly in the area of structure, synthesis and processing, characterisation, advanced-state properties and applications of materials. All published articles are indexed in various databases and are available download for free. The manuscript management system is completely electronic and has fast and fair peer-review process. The journal includes review article, research article, notes, letter to editor and short communications.

Copyright © 2017 VBRI Press AB, Sweden

www.vbripress.com/aml